Supporting Information

Leonetti et al. 10.1073/pnas.1215078109

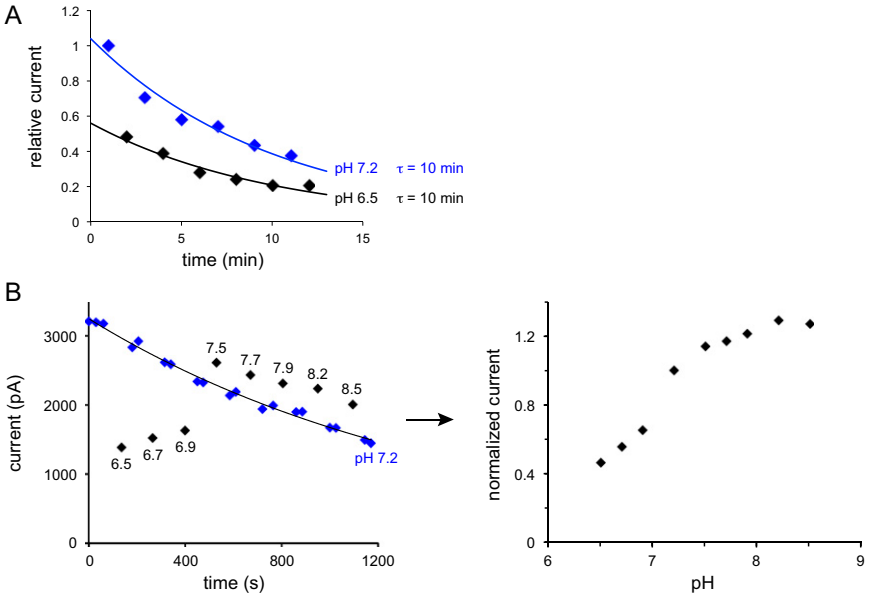

Fig. S1. Rundown of hSLO3+LRRC52 currents. (*A*) Current (at +180 mV) from a single inside-out patch bathed sequentially in solutions of pH 7.2 and pH 6.5 over time. Values are normalized to the first measurement (1 min; pH 7.2). Solid lines correspond to exponential fits: $I(t) = A*\exp(-t/\tau)$. The time constant τ is the same at both values of pH. For pH 7.2, A is $1.04 \pm 5.9 \times 10^{-2}$ and τ is 10 ± 1.2 min. For pH 6.5, A is $0.57 \pm 3.8 \times 10^{-2}$ and τ is 10 ± 1.1 min. (*B*) pH titration of hSLO3+LRRC52 currents. The example is shown of currents (at +180 mV) recorded from a single inside-out patch at different values of pH (*Left*). Measurements at pH 7.2 provide a baseline to evaluate the effect of rundown (solid line, exponential fit). All measurements are then normalized to this baseline to obtain the pH titration curve shown (*Right*). This analysis allows a better estimate of the pH sensitivity of hSLO3+LRRC52 currents but does not distinguish between the two possible causes of rundown: loss of channels or change in gating properties. If rundown reflects a change in gating properties over time, the pH sensitivity we measure could represent the functional properties of a heterogeneous population of channels. Therefore, our measurements might not comprehensively describe the pH dependence of hSLO3+LRRC52 currents but clearly underscore the pronounced effect of LRRC52: upon coexpression with LRRC52, the range of pH at which hSLO3 currents open is substantially shifted to lower values.

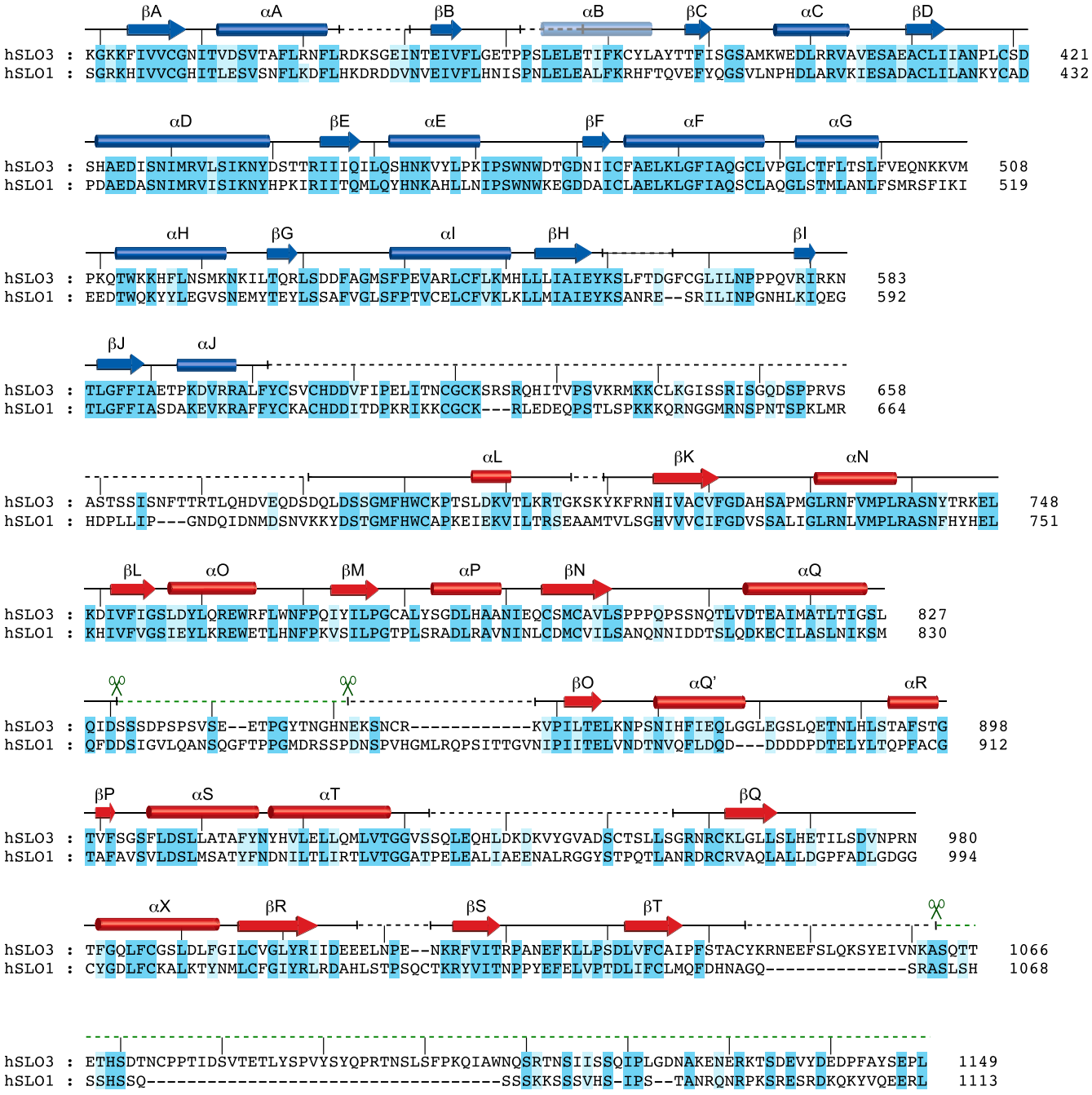

Fig. S2. Sequence alignment of the cytoplasmic domains from human SLO3 and SLO1 channels. Amino acid conservation is indicated in blue shadings. Secondary structure elements present in the hSLO3 gating ring structure are shown, keeping the same nomenclature as for SLO1 (helix αB is shown, even though the electron density in this region is poor). Disordered, nonmodeled regions in the hSLO3 structure are shown in dashed lines. The loop and C-terminal deletions used for structure determination are indicated by scissors.

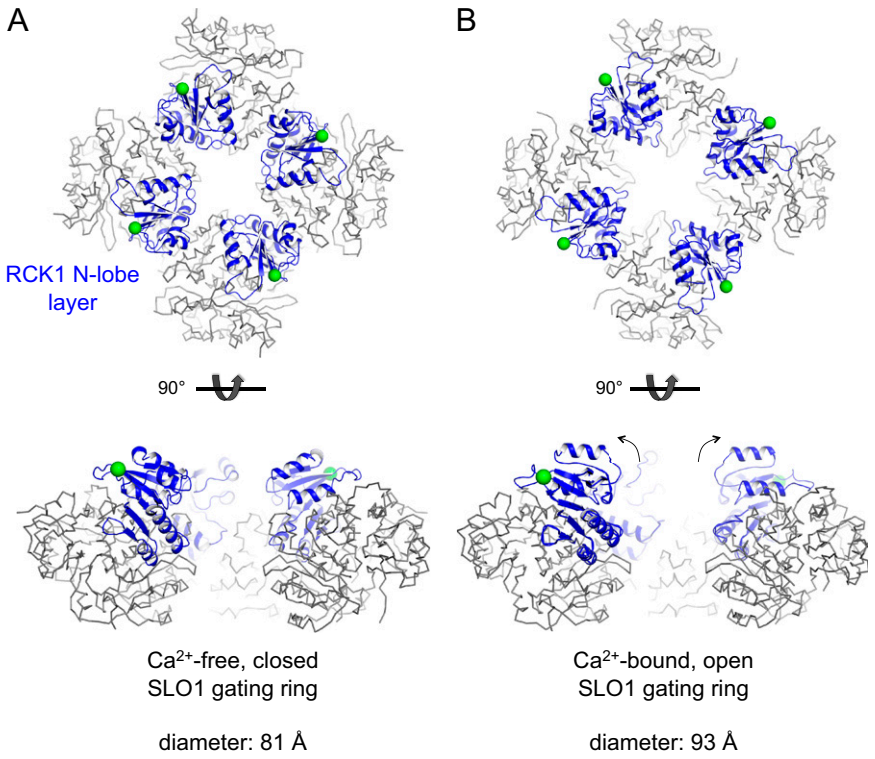

Fig. S3. RCK1 N-lobe conformational changes between the open and closed conformations of the SLO1 gating ring. (*A*) Structure of the Ca^{2+}-free, closed SLO1 gating ring (PDB ID code 3NAF). The RCK1 N-lobes from all four subunits ("RCK1 N-lobe layer") are in blue; RCK1 N-termini (Lys-343) are shown as green spheres. *Lower*: Front subunit is removed for clarity. (*B*) Same as in *A*, showing the Ca^{2+}-bound, open structure of the SLO1 gating ring (PDB ID code 3U6N). The major conformational change upon Ca^{2+} binding involves the RCK1 N-lobe layers, which "open up," leading to an increase of the ring's diameter (measured from the N termini of opposing subunits).

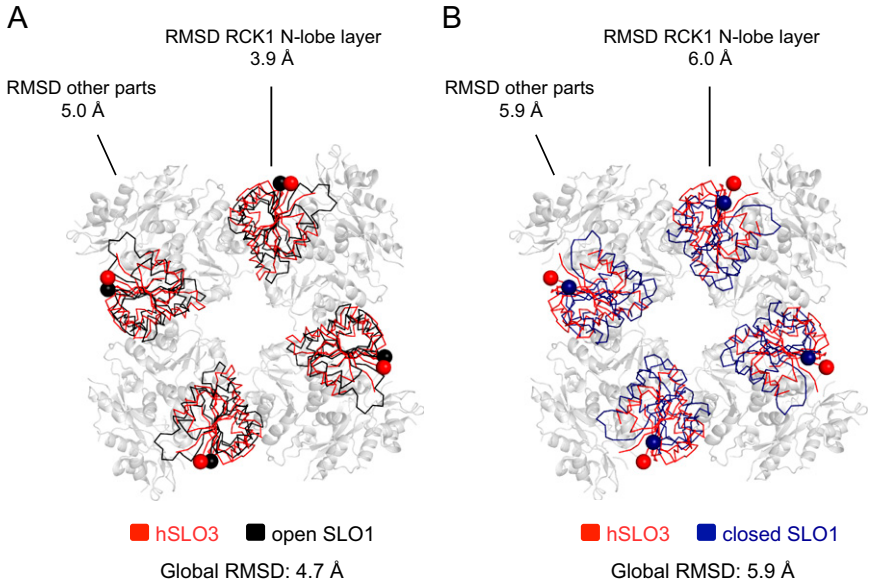

Fig. S4. All-Cα atom superpositions of the hSLO3 and SLO1 gating rings. (*A*) Objective superposition of the hSLO3 and open SLO1 gating rings by aligning all Cα atoms from the tetrameric structures. The RCK1 N-lobe regions from all four subunits (i.e., RCK1 N-lobe layer) of the hSLO3 (red) and open SLO1 (black) gating rings are shown as a ribbon. The rest of the structure, where the superposition is poor and is not shown, is drawn as a gray cartoon. RCK1 N-terminal residues (K332 in hSLO3, K343 in SLO1) are shown as spheres. (*B*) Same as in *A* but showing the superposition of the hSLO3 and closed SLO1 gating rings.

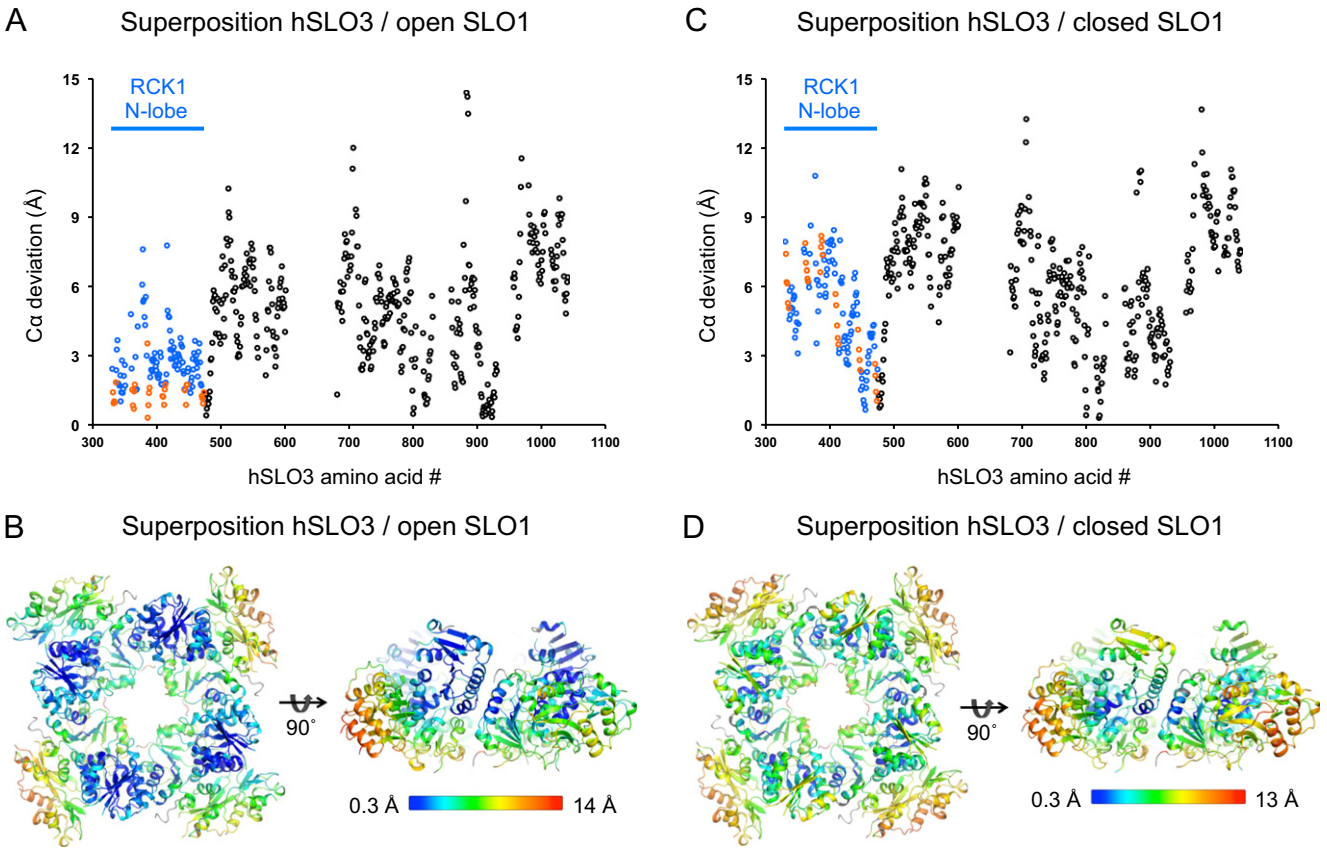

Fig. S5. Deviations between individual Cα atoms in the superpositions shown in Fig. 5. In these superpositions, the hSLO3 and open or closed SLO1 gating ring structures were aligned by using the Cα atoms of the RCK1 N-lobes from all four subunits. Here we plot the distances between corresponding hSLO3 and SLO1 Cα atoms ("Cα deviations") in these superpositions. (*A*) Plot of Cα deviations between the hSLO3 and open SLO1 gating ring structures for individual hSLO3 amino acids. Amino acids in the RCK1 N-lobe region are shown in blue, with residues forming the central RCK1 N-lobe β-sheet highlighted in orange. (*B*) hSLO3 gating ring structure colored according to the Cα deviations of individual amino acids in the superposition between hSLO3 and the open conformation of SLO1. (*C* and *D*) Same as in *A* and *B*, but illustrating the superposition between hSLO3 and the closed conformation of SLO1.

Table S1. X-ray data collection and processing

Datasets	Dataset 1	Dataset 2	Merged dataset
Resolution, Å	45–3.3	50–3.4	50–3.3
Space group	I222	I222	I222
Source	BNL X29	BNL X29	—
Cell constants, Å			
a	124.10	124.53	124.54
b	158.90	157.94	157.94
c	248.27	249.00	249.00
α, β, γ, °	90, 90, 90	90, 90, 90	90, 90, 90
Wavelength, Å	1.075	1.29	—
Completeness, %	99.6 (100)	99.7 (100)	99.9 (100)
R_{merge}	0.081 (0.810)	0.095 (0.957)	0.124 (>1)
Unique reflections	37,405	35,337	36,517
I/σ(I)	15.9 (1.6)	12.5 (1.3)	15.0 (1.8)
Redundancy	4.8 (4.8)	3.5 (3.4)	8.3 (8.3)

Numbers in parenthesis represent values in the highest-resolution shell.

Table S2. Structure refinement statistics

Refinement (after anisotropic correction)	
Resolution, Å	48.5–3.4[†]
a*	3.8
b*	3.4
c*	3.4
Completeness, %	89.9 (38.6)
R_{work}	0.248 (0.322)
R_{free}	0.267 (0.276)
No. of atoms (protein)	8,241
Average B factors, Å^2	68.3
Ramachandran plot	
Favored/allowed/disallowed, %	96.5/3.5/0
rmsd bond lengths, Å	0.007
rmsd bond angles, °	1.026

Numbers in parentheses represent values in the highest-resolution shell; R_{free} was calculated with 5% of the data.

[†]Reflections beyond these limits were excluded from refinement after anisotropic correction (a*, b*, and c* indicate reciprocal cell directions).